ResearchGate

See discussions, stats, and author profiles for this publication at: https://www.researchgate.net/publication/6211999

Electronic Structures and Conductivity in Peptide Nanotubes

ARTICLE *in* THE JOURNAL OF PHYSICAL CHEMISTRY B · SEPTEMBER 2007

Impact Factor: 3.3 · DOI: 10.1021/jp0708446 · Source: PubMed

CITATIONS
8

READS
23

3 AUTHORS, INCLUDING:

Hong Wang
West Virginia University
24 PUBLICATIONS **735** CITATIONS
SEE PROFILE

James P Lewis
West Virginia University
90 PUBLICATIONS **2,798** CITATIONS
SEE PROFILE

Available from: James P Lewis
Retrieved on: 02 February 2016

Electronic Structures and Conductivity in Peptide Nanotubes

R. Takahashi,[‡] H. Wang,*[,†] and J. P. Lewis[†]

Department of Physics and Astronomy, Brigham Young University, Provo, Utah 84602, and Department of Physics, West Virginia University, Morgantown, West Virginia 26506

Received: January 31, 2007; In Final Form: May 7, 2007

Self-assembling cyclic D,L-peptide nanotubes are electronically insulating and possess wide band gaps (E_g > 4eV). Our ab initio electronic structure calculations indicate that the presence of aromatic rings in the side chain of peptide nanotubes significantly reduces the band gap. We investigate the conductivity of the modified peptide nanotubes through calculations of the electron tunneling probability. The electron tunneling probability through a molecule depends on the length of the molecule, L, as $e^{-\beta(E)L}$, where the tunneling $\beta(E)$-factor is strongly energy-dependent. We have calculated $\beta(E)$ in three types of peptide nanotubes that have different sequences of amino acid residue, (L-Gln, D-Ala)$_4$, (L-Gln, D-Leu)$_4$ and (L-Gln, D-Phe)$_4$, using the complex band structure approach. We find large β values near midgap, making these peptide nanotubes a poor tunneling conductor.

I. Introduction

Peptide nanotubes (PNTs) are open-ended, hollow, tubular structures that are self-assembled through stacking of appropriately designed cyclic peptide subunits. These structures constitute a unique class of self-organized biomaterials with tunable surface characteristics and internal diameters.[1−8] PNTs have a wide range of functional attributes that are useful in biological[2,3,9,10] and material science.[11−15]

As a result of increasing interest in the field of molecular electronics,[16−21] theoretical calculations have been used to assess the conductive properties of self-assembling PNTs.[22−28] Self-assembling cyclic D,L-PNTs are electronically insulating, as are most biomaterials derived from natural amino acids. It has been proposed that the cyclic D,L-PNTs should possess wide band gaps (E_g > 4 eV) that could potentially be tuned through appropriate modification of the cyclic peptide.[26] However, the natural amino acid side chains are not sufficient to create electronically conductive assemblies. Recently, Ghadiri et al. proposed that, in the D,L-α-PNTs, cyclic peptide self-assembly might be useful in controlling and directing the stacking of aromatic side chains and might offer a level of control over the long-range order in the resulting materials.[13,29]

In this work, three types of D,L-PNTs are chosen to study the side chain effects on the electronic structures and conductivity in PNTs. These PNTs consist of L-glutamine and three different D-amino acids: D-alanine, D-leucine, and D-phenylalanine.[5] The detailed structural properties of these PNTs are summarized in Section II, the computational method is discussed in Section III, and the results of the electronic structures and conductivity in the periodic PNTs are presented in Section IV. A short section of conclusions closes this paper.

II. Structure Properties of the PNT

The PNTs used in our calculations are synthesized in the experiments done by Ghadiri's group through the following mechanisms.[5] First, hydrogen bonding is a driving force of synthesis in PNTs. Glutamine is used in the structure because it is a polar amino acid, having hydrogen-bonding donor/acceptor capability in its amide side chains. Therefore, it can contribute in the formation of PNTs. Second, PNTs are synthesized assuming the hypothesis that hydrophobic interactions play the dominant part in the orientation of nanotubes. The hydrophobic character is important because PNTs are formed in aqueous solution. If amino acid residues are to have no interaction with water molecules, hydrogen bonding between the peptide subunit is strengthened, making formation of the PNTs easier.

Each of the PNTs in this study is a combination of L-glutamine with hydrophobic amino acid residues. These PNTs are combinations of L-glutamine and three different D-amino acids: D-alanine, D-leucine, and D-phenylalanine. Four sets of alternating L- and D-amino acid residues make the model PNTs contain eight residue peptide rings. The fundamental unit of PNTs is a cyclic peptide ring. Experiments have shown that the PNTs are synthesized in a set of two rings called dimers.[5] Each peptide ring in the dimer stacks in an antiparallel way. Therefore, for the purposes of our calculations, we choose a dimer as the unit cell and utilize periodic boundary conditions. The top and side view of the dimer, the building block of the three PNTs studied, are illustrated in Figures 1, 2, and 3, respectively. Dimers consisting of (L-Gln, D-Ala)$_4$, (L-Gln, D-Leu)$_4$ and (L-Gln, D-Phe)$_4$ contain 216, 288, and 296 atoms, respectively. We call these periodic PNTs QA$_4$, QL$_4$, and QF$_4$, respectively, throughout the rest of this paper. The distances between the subunit and the dimer of these PNTs are summarized in the Table 1 (see ref 5 for the details).

III. Computational Methods

The complex band structure of a periodic system is the conventional band structure extended to complex Bloch k-vectors. In a "conventional" band structure calculation, one inputs a k-vector for a propagating state using Bloch's theorem and solves the Schrödinger equation for eigenvalues of energy E. In contrast, the complex band structure inputs the energy E, and the output is the k-vector (now complex) that produces this

[†] West Virginia University.
[‡] Brigham Young University.

10.1021/jp0708446 CCC: $37.00 © 2007 American Chemical Society
Published on Web 07/11/2007

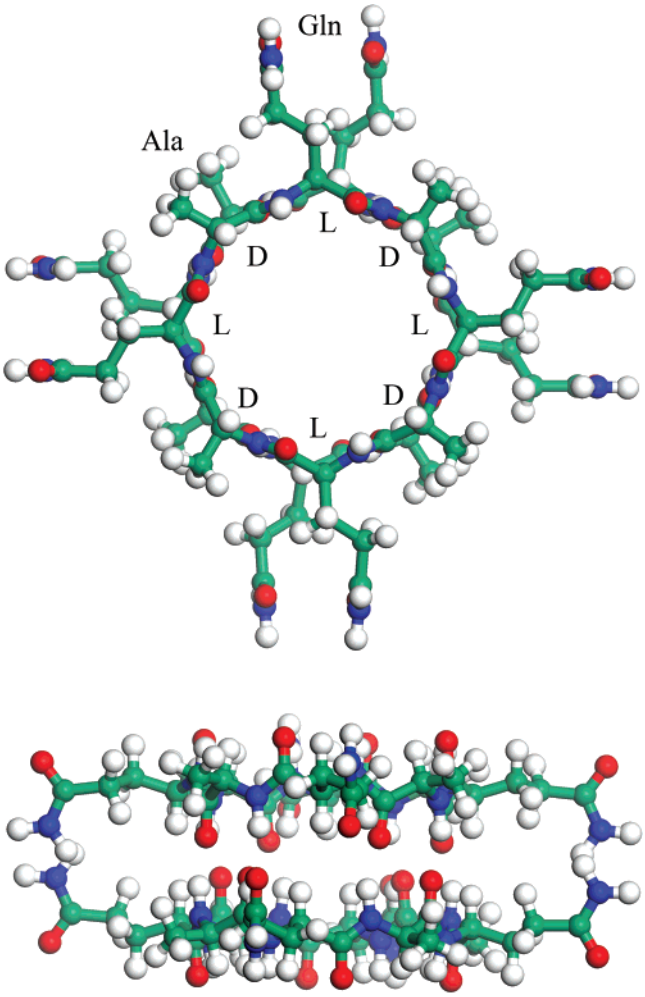

Figure 1. Top view and side view of the dimer, the building block of the (L-Gln, D-Ala)$_4$ nanotube.

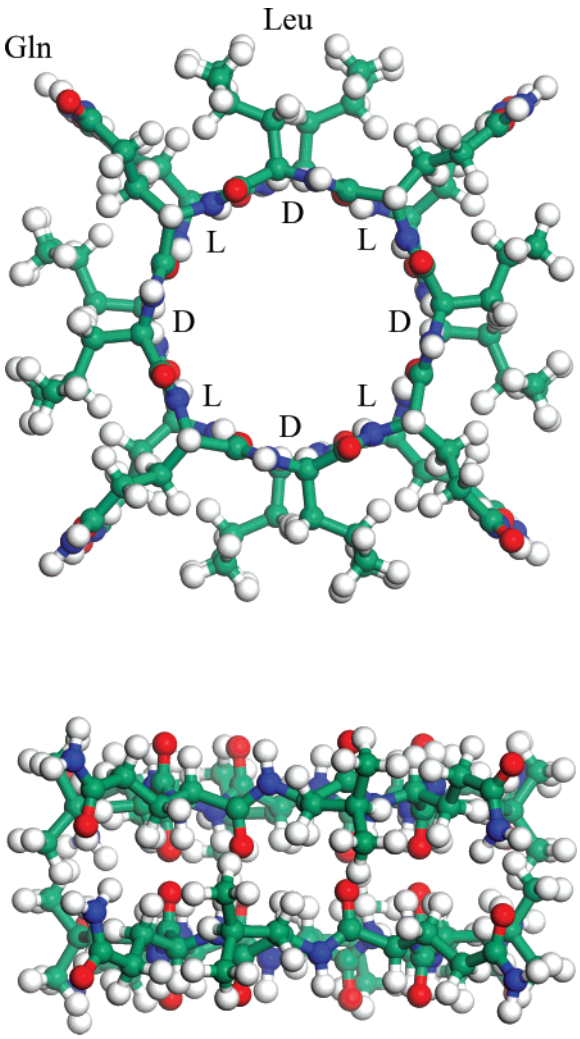

Figure 2. Top view and side view of the dimer, the building block of the (L-Gln, D-Leu)$_4$ nanotube.

energy. A generalization of Bloch's theorem is used that allows the wavefunction to decay or increase as one moves from periodic cell to cell. References 30−33 give the mathematical details.

The Bloch k-vectors with an imaginary part describe spatially decaying wave functions and arise in, for example, the analysis of impurity and surface states.[34,35] They also represent the quantum tunneling states that are vehicles of electron (hole) transport through a barrier, such as a thin oxide layer or a molecule. For example, in a simple square barrier, the tunneling probability is approximately equal to $e^{-2\kappa L}$, where $\kappa = \sqrt{(2m/\hbar^2)(V_0-E)}$ is the imaginary part of the Bloch k-vector, L is the length of the barrier, and the factor of 2 in the exponent comes from squaring the wave function. Analogous to a simple square barrier, for complex Bloch k states, the tunneling probability will be $\sim e^{-\beta L}$, where $\beta = 2\mathrm{Im}(k)$ and β is a function of energy. The previous reports regarding conductivity in molecular electronics indicated that much of the experimental work has focused on current−voltage characteristics. These experiments are likely sensitive to a number of variables not directly related to the molecule (e.g., the nature of the contacts or the chemical environment). A key advantage of the complex band structure approach is that it takes the contacts (electrodes) and other environmental variables out of the system. The complex band structure tells us about conduction characteristics that are solely intrinsic to the molecule.

In this work, we investigate the tunneling decay $\beta(E)$-factor of PNTs, which is obtained from the complex band structure method.[30−33] The transmission probability of a charge is proportional to $e^{-\beta(E)L}$, where L is the tunneling distance. Our analysis here is for the periodic PNTs. Both the complex and real band structures are calculated using an ab initio tight-binding method, called FIREBALL, which is based on density functional theory with a nonlocal pseudopotential scheme.[36−38] FIREBALL is a first-principles, tight-binding molecular dynamics simulation technique based on a self-consistent version of the Harris−Foulkes[39,40] functional. In this method, confined atomic-like orbitals are used as a basis set for the determination of the occupied eigenvalues and eigenvectors of the one-electron Hamiltonian. The "fireball" orbitals, introduced by Sankey and Niklewski,[41] are obtained by solving the atomic problem with the boundary condition that the atomic orbitals vanish outside and at a predetermined radius, r_c, where wavefunctions are set to be zero. This boundary condition is equivalent to an "atom in the box" and has the effect of raising the electronic energy levels due to confinement. An important advantage of the Sankey and Niklewski basis set is that the Hamiltonian and the overlap matrix elements of the system are quite sparse for large systems, reducing overall computation time. On the other hand, the light excitation of the atoms somewhat accounts for Fermi compression in solid, which apparently gives a better representation of solid-state charge densities.[42] This method has already

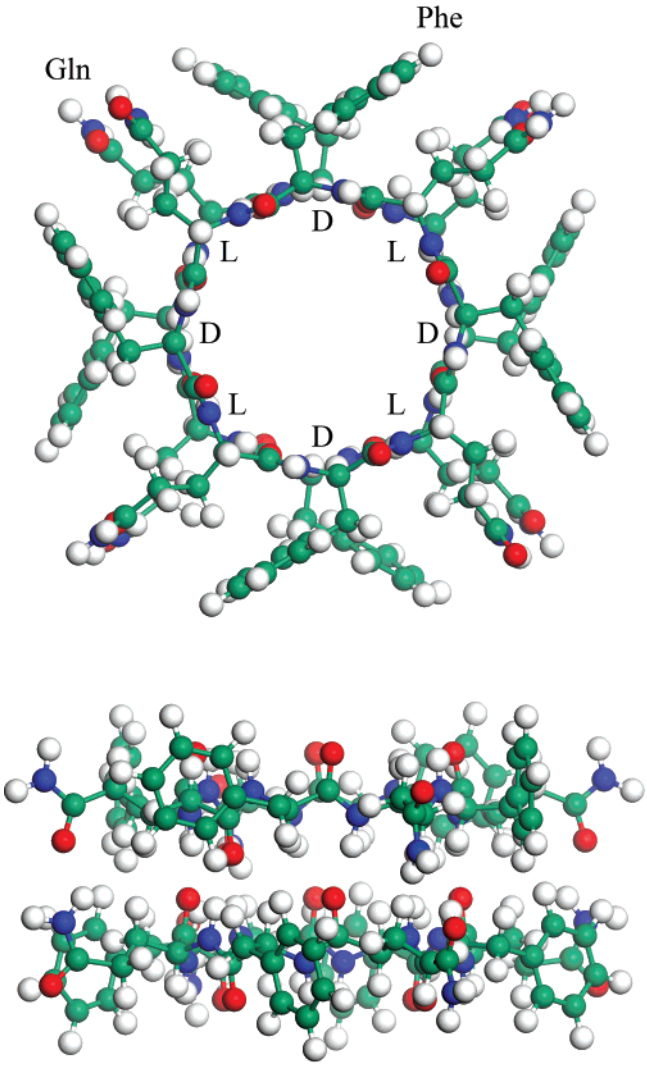

Figure 3. Top view and side view of the dimer, the building block of the (L-Gln, D-Phe)$_4$ nanotube.

TABLE 1: Structure Properties of the PNTs[5]

	(L-Gln, D-Ala)$_4$	(L-Gln, D-Leu)$_4$	(L-Gln, D-Phe)$_4$
nos. of atom	216	288	296
subunit distance (Å)	4.74	4.72	4.73
dimer distance (Å)	9.60	9.50	9.66

been used with success in a variety of inorganic systems and biomolecules.[36−38,43,44] In this work, we use the Becke exchange[45] with Lee−Yang−Parr correlation.[46] We have adopted the double numerical basis sets[47−50] for C, N, and O to yield higher accuracy and correct polarization, whereas a minimal basis set is used for H.

IV. Results

The band structure (for both complex and real k) of the QA$_4$, QL$_4$, and QF$_4$ PNTs are presented in Figure 4a, b, and c, respectively. The right panels show regions where the k-vector is entirely real, representing the conventional band structure. The left panels show $\beta(E)$, which is twice the imaginary part of $k(E)$ for all energies E. We first discuss the conventional band structures of the PNTs. From the right panel of Figure 4a, we see that the QA$_4$ PNTs are analogous to semiconducting material with a band gap of 4.08 eV and the valance band edge occurs at $k = \pi/a$. A similar semiconducting-like behavior is

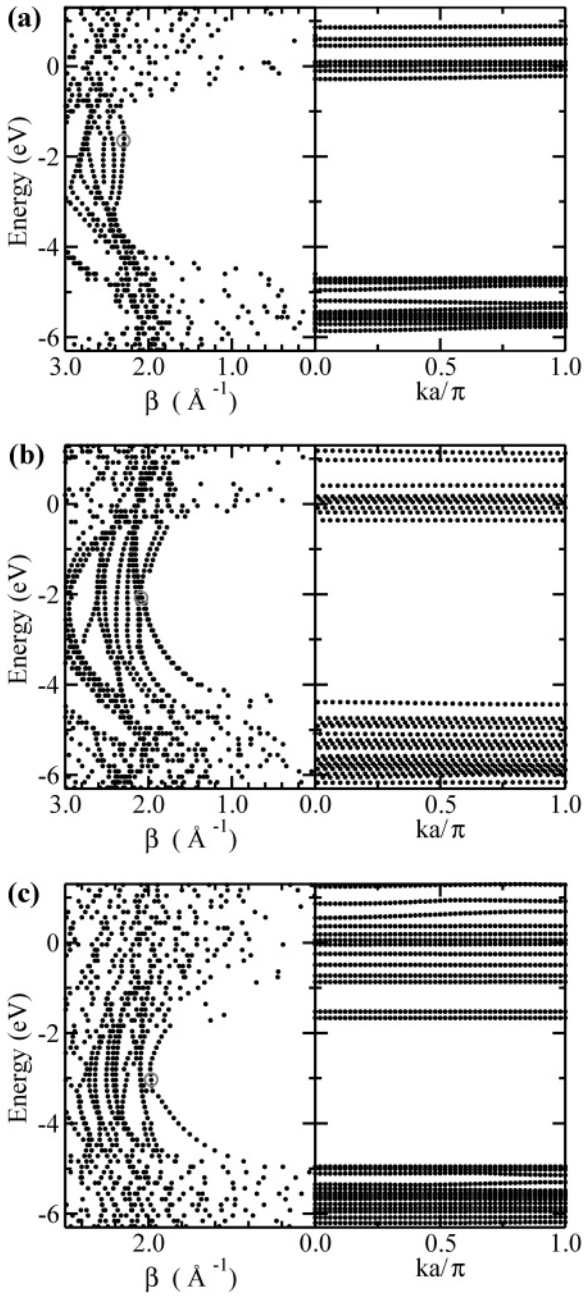

Figure 4. The complex band structure for (a) QA$_4$, (b) QL$_4$, and (c) QF$_4$ PNTs, respectively. The right panel shows the conventional band structure, $E(k)$, for real k vectors along the PNTs dimer, and the left panel shows the complex band structure $k(E)$, where only the imaginary part of k, $\beta(E)$, is shown. The red circles in the left panels indicate the branch points of the systems.

found in the QL$_4$ PNTs, which have a smaller band gap of 3.95 eV (see right panel of Figure 4b). The band gap of the QA$_4$ and QL$_4$ PNTs are consistent with previous calculations.[22−26] However, the strong side chain effects on the electronic structure of PNTs is observed in the QF$_4$ structure, where the band gap of 2.94 eV is obtained.

The major structure difference between the QF$_4$ nanotube and the other two nanotubes (QA$_4$ and QL$_4$) is the existence of aromatic rings in the side chains in the QF$_4$ PNTs. Using aromatic rings as molecular wires in the molecular electronics is desirable because the π conjugate characteristics in the aromatic rings can be delocalized along the length of the molecules.[13,21,29] There is no strong covalent bonding expected in the QF$_4$ PNTs, since the aromatic rings in the phenylalanine

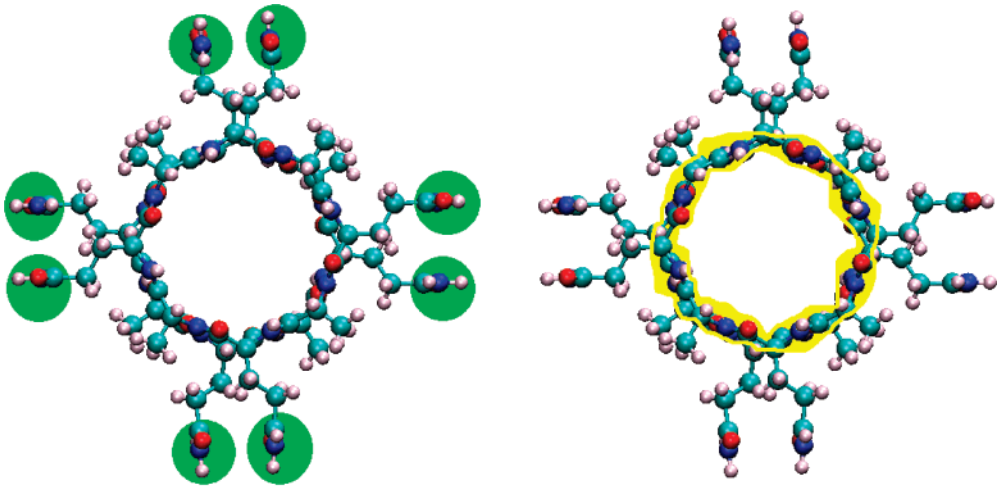

Figure 5. Population densities for (a) the HOMO state and (b) the LUMO state are shown for the QA_4 PNTs, respectively.

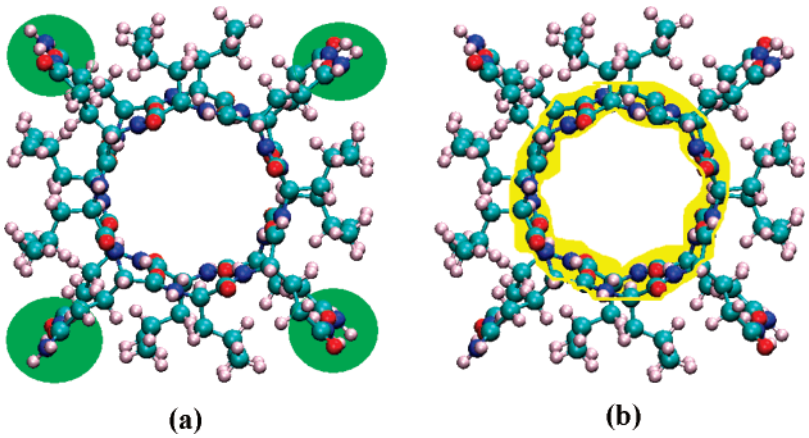

Figure 6. Population densities for (a) the HOMO state and (b) the LUMO state are shown for the QL_4 PNTs, respectively.

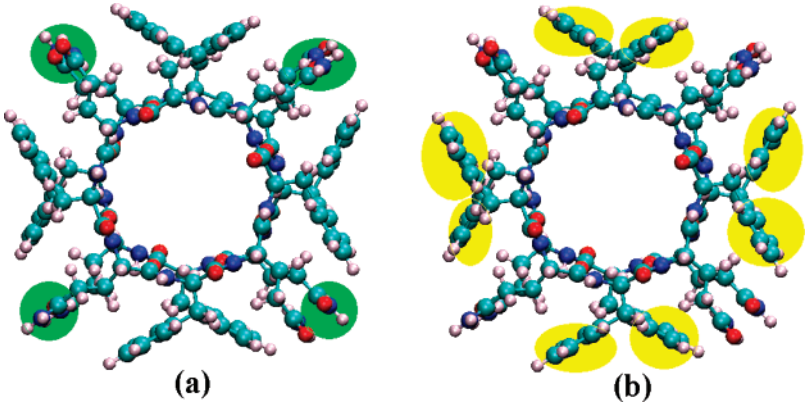

Figure 7. Population densities for (a) the HOMO state and (b) the LUMO state are shown for the QF_4 PNTs, respectively.

side chains are separated by a large distance of 4.73 Å. However, the weak π conjugate systems due to the existence of aromatic rings in the phenylalanine side chains are likely the cause of band gap narrowing in the QF_4 PNTs. Additionally, the orientation of each aromatic ring within the molecule should also be considered; an orientation that preserves the π conjugate system will allow delocalization of electrons along the length of molecular chain. Therefore, having better aligned and closer staked aromatic rings in the PNTs side chain, such as phenylalanine and tyrosine, will enhance its conductivity.

Within the band gap, there are no propagating states, but rather, only exponential tunneling states. The amount of tunneling is controlled by the $\beta(E)$ curve. Within the fundamental band gap between the valence and conduction bands, there are several $\beta(E)$ curves. Since the tunneling probability decays as $e^{-\beta}L$ (L is the distance along the length of molecule), the states with large β values do not play a significant role in conduction. In particular, we only need to consider the smallest β states, described by the semielliptical-like curve in the band gap energy region. This branch produces the most penetrating state and overwhelmingly dominates tunneling. The curve $\beta(E)$ reaches a maximum value near midgap. This maximum is called the branch point, which is approximately where the wave function changes from valence-band character (bonding) to

conduction-band character (antibonding). For the purpose of definiteness, we identify the branch point as being that point where the β value reaches a maximum, and $dE/d\beta \rightarrow \infty$. In the left panel of Figure 4, the red circle indicates the branch point in the PNTs studied. The branch point β (E) value for the QA_4 PNTs is $\beta_{bp} = 2.28$ Å^{-1} ($E_{bp} = -1.65$ eV), whereas those for the QL_4 and QF_4 are $\beta_{bp} = 2.09$ Å^{-1} ($E_{bp} = -2.08$ eV) and $\beta_{bp} = 1.96$ Å^{-1} ($E_{bp} = -3.03$ eV), respectively.

In molecular electronics, metallic contacts are made at two ends of the molecule, and electronic current is expected to be carried by electrons tunneling from the metal with energies in the band gap region. The branch point plays an important role in the analysis of the electron transport properties. The branch point energy, E_{bp}, is an estimate for the lineup of the metal Fermi level (E_F) with the molecular levels, and $\beta_{bp} = \beta(E_{bp})$ provides the tunneling decay rate. We now use this information to obtain a simple estimate of the conductance of a molecule. According to Landauer theory,[51] when E_F crosses a propagating molecular state (such as the highest occupied molecular orbital) in the real k region of the complex band structure, the low-voltage conductance of the molecule will be approximately equal to the quantum of conductance, $G_0 \approx 77$ μS. However, E_F will lie in the band gap, and the conductance, g, will be reduced from its value of G_0 by the approximate factor $e^{-\beta_{bp}L}$, where β_{bp} is the β value of the most penetrating gap state at the Fermi level, E_F, and L is the length of the molecule. Using these approximations, the estimated conductance is given by $g \approx G_0 e^{-\beta_{bp}L}$.

Let us consider electron tunneling through a dimer ($L = 9.66$ Å) of the QF_4 PNTs, which has the smallest $\beta_{bp} = 1.96$ Å^{-1}; then the estimated conductance is $g(QF_4) = G_0 e^{-\beta_{bp}L} = 4.61 \times 10^{-7}$ μS. For the other two PNTs, QA_4 ($L = 9.60$ Å) and QL_4 ($L = 9.50$ Å), the estimated conductances we obtained while electron-tunneling through a dimer were $g(QA_4) = 2.40 \times 10^{-8}$ μS and $g(QL_4) = 1.83 \times 10^{-7}$ μS, respectively. We can compare this to a "typical" organic molecule wired in a molecular electronics experiment. Specifically, consider (i) alkenes, $(CH)_n$, a zigzag conjugated chain with alternating single and double bonds between carbon atoms; and (ii) alkanes, $(CH_2)_n$, a zigzag chain of single sp^3 bonds between carbon atoms. The estimated conductance for an alkene chain ($\beta = 0.27$ Å^{-1} with a narrow band gap of 1.9 eV)[30] of length $L \approx 10$ Å gives g (alkane) ≈ 5.2 μS. Similarly, for an alkane chain of the same length ($\beta = 0.79$ Å^{-1} with a very wide band gap near 10 eV[30]) gives g (alkane) $\approx 2.9 \times 10^{-2}$ μS.

What we have learned from the above comparison is how poor PNTs are as a conductor through "conventional" band gap tunneling and how important the β is in determining the conductivity of the systems. The larger β obtained in the PNTs results from the PNTs being formed by the means of hydrogen bonding, which has smaller orbital overlap compared with covalent bonding. A similar phenomenon is observed in our previous study of DNA conductivity.[43] There, the branch point β value of $\beta_{bp} = 1.5$ Å^{-1} is obtained for both poly(dA)−poly(dT) and poly(dG)−poly(dC) periodic DNA double helices, and the estimated conductance for electron tunneling through 3-base pairs ($L \approx 10$ Å) is g (DNA) $\approx 2.4 \times 10^{-5}$ μS.[43] However, significant modification of the PNTs by adding the better aligned and closer staked aromatic rings should improve their electronic conductivity for use as molecular wires.[15,24]

To investigate the charge distribution in the PNTs for states near the fundamental band gap, we calculate the population densities in the PNTs. From a particular state ν, the wavefunction $\psi(\nu)$ has a Mulliken population $p_k(\nu)$ on atom k, which loosely is considered the probability that an electron in state ν resides on a particular atom k. The populations are normalized, $\sum_k p_k(\nu) = 1$. The population density for the highest occupied molecular orbital (HOMO) in the QA_4 PNTs is plotted in Figure 5a, whereas that for the lowest unoccupied molecular orbital (LUMO) is plotted in Figure 5b. The results for the QL_4 and QF_4 PNTs are represented in Figure 6 and Figure 7, respectively. In these figures, the population density of the HOMO state is illustrated by the green areas, whereas the yellow areas represent the population density of the LUMO state. Figure 5a and b show that the HOMO state resides on the glutamine side chains and the population density of the LUMO state resides on the backbone of the cyclic peptide in the QA_4 PNTs. Similar results are obtained in the QL_4 PNTs through the observation of Figure 6. However, for the QF_4 PNTs (Figure 7), we see that the population density of the HOMO state resides on the glutamine side chains and the population density of the LUMO state resides on the phenylalanine side chains. From these results, we ascertain that the choice of side chains not only causes the band gap energy to change but also significantly affects the conduction state wavefunctions.

V. Conclusion

In summary, the complex band structure of the three types of PNTs has been evaluated to obtain the energy dependence of the tunneling decay constant $\beta(E)$ in PNTs. The electronic structure calculations show that PNTs have semiconductor-like band gaps. We predict the electron-transfer rate for electron energies near midgap with a decay constant of $\beta = 2.28$, 2.09, and 1.96 Å^{-1} in (L-Gln, D-Ala)$_4$, (L-Gln, D-Leu)$_4$, and (L-Gln, D-Phe)$_4$ PNTs, respectively. Compared with other organic molecules, we find that these PNTs are poor tunneling, wide-gap, semiconductor-like organic molecules. On the basis of our calculations, we conclude that these PNTs do not generally exhibit good "molecular wire" characteristics.

Acknowledgment. The atomic structures of the PNTs studied in this work are provided by Dr. Ashkenasy from the Scripps Research Institute. We are also grateful to N. Ashkenasy, R. Davis and O. F. Sankey for helpful discussions. These calculations were run at the Ira and Mary Lou Fulton Supercomputing Laboratory.

References and Notes

(1) Ghadiri, M. R.; Granja, J. R.; Milligan, R. A.; McRee, D. E.; Khazanovich, N. *Nature* **1993**, *366*, 324.
(2) Ghadiri, M. R.; Granja, J. R.; Buehler, L. K. *Nature* **1994**, *369*, 301.
(3) Khazanovich, N.; Granja, J. R.; McRee, D. E.; Milligan, R. A.; Ghadiri, M. R. *J. Am. Chem. Soc.* **1994**, *116*, 6011.
(4) Ghadiri, M. R. *Adv. Mater.* **1995**, *7*, 675.
(5) Hartgerink, J. D.; Granja, J. R.; Milligan, R. A.; Ghadiri, M. R. *J. Am. Chem. Soc.* **1996**, *118*, 43.
(6) Clark, T. D.; Buehler, L. K.; Ghadiri, M. R. *J. Am. Chem. Soc.* **1998**, *120*, 651.
(7) Bong, D. T.; Clark, T. D.; Granja, J. R.; Ghadiri, M. R. *Angew. Chem., Int. Ed.* **2001**, *40*, 988.
(8) Fernandez-Lopez, S.; Kim, H.-S.; Choi, E. C.; Delgado, M.; Granja, J. R.; Khasanov, A.; Kraehenbuehl, K.; Long, G.; Weinberger, D. A.; Wilcoxen, K. M.; Ghadiri, M. R. *Nature* **2001**, *412*, 452.
(9) Sanchez-Quesada, J.; Kim, H. S.; Ghadiri, M. R. *Angew. Chem.* **2001**, *113*, 2571.
(10) Sanchez-Quesada, J.; Isler, M. P.; Ghadiri, M. R. *J. Am. Chem. Soc.* **2002**, *124*, 10004.
(11) Vollmer, M. S.; Clark, T. D.; Steinem, C.; Ghadiri, M. R. *Angew. Chem.* **1999**, *111*, 1703.
(12) Vollmer, M. S.; Clark, T. D.; Steinem, C.; Ghadiri, M. R. *Angew. Chem., Int. Ed.* **1999**, *38*, 1598.
(13) Steinem, C.; Janshoff, A.; Vollmer, M. S.; Ghadiri, M. R. *Langmuir* **1999**, *15*, 3956.
(14) Motesharei, K.; Ghadiri, M. R. *J. Am. Chem. Soc.* **1997**, *119*, 11306.

(15) Horne, W. S.; Stout, C. D.; Ghadiri, M. R. *J. Am. Chem. Soc.* **2003**, *125*, 9372.
(16) Bachtold, A.; Hadley, P.; Nakanishi, T.; Dekker, C. *Science* **2001**, *294*, 1317.
(17) Collier, C. P.; Mattersteig, G.; Wong, E. W.; Luo, Y.; Beverly, K.; Sampaio, J.; Raymo, F. M.; Stoddart, J. F.; Heath, J. R. *Science* **2000**, *289*, 1172.
(18) Huang, Y.; Duan, X.; Wei, Q.; Lieber, C. M. *Science* **2001**, *291*, 630.
(19) Joachim, C.; Gimzewski, J. K.; Aviram, A. *Nature* **2000**, *408*, 541.
(20) Tour, M. *J. Acc. Chem. Res.* **2000**, *33*, 791.
(21) Reed, M. A. Molecular Electronics—Current Status and Future Prospectus; *FED J.* **2000**, *11*, 57.
(22) Carloni, P.; Andreoni, W.; Parrinello, M. *Phys. Rev. Lett*. **1997**, *79*, 761.
(23) Lewis, J. P.; Pawley, N. H.; Sankey, O. F. *J. Phys. Chem. B* **1997**, *101*, 10576.
(24) Jishi, R. A.; Braier, N. C.; White, C. T.; Mintmire, J. W. *Phys. Rev. B: Condens. Matter Mater. Phys.* **1998**, *58*, R16009.
(25) Okamoto, H.; Takeda, K.; Shiraishi, K. *Phys. Rev. B: Condens. Matter Mater. Phys.* **2001**, *64*, 115425.
(26) Okamoto, H.; Nakanishi, T.; Nagai, Y.; Kasahara, M.; Takeda, K. *J. Am. Chem. Soc.* **2003**, *125*, 2756.
(27) Horne, W. S.; Ashkenasy, N.; Ghadiri, M. R. *Chem.—Eur. J.* **2005**, *11*, 1137.
(28) Ashkenasy, N.; Horne, W. S.; Ghadiri, M. R. *Small* **2006**, *2*, 99.
(29) Rapaport, H.; Kim, H. S.; Kjaer, K.; Howes, P. B.; Cohen, S.; Als-Nielsen, J.; Ghadiri, M. R.; Leiserowitz, L.; Lahav, M. *J. Am. Chem. Soc.* **1999**, *121*, 1186.
(30) Boykin, T. B. *Phys. Rev. B: Condens. Matter Mater. Phys.* **1996**, *54*, 7670.
(31) Boykin, T. B. *Phys Rev. B: Condens. Matter Mater. Phys.* **1996**, *54*, 8107.
(32) Tomfohr J. K.; Sankey, O. F. *Phys. Rev. B: Condens. Matter Mater. Phys.* **2002**, 245105 and references therein.
(33) Tomfohr, J. K.; Sankey, O. F. *Phys. Stat. Solidi B* **2002**, *233*, 59.
(34) Heine, V. *Phys. Rev.* **1965**, *138*, A1689.
(35) Rehr, J. J.; Kohn, W. *Phys. Rev. B: Condens. Matter Mater. Phys.* **1974**, *9*, 1981.
(36) Demkov, A. A.; Ortega, J.; Sankey, O. F.; Grumbach, M. P. *Phys. Rev. B: Condens. Matter Mater. Phys.* **1995**, *52*, 1618.
(37) Lewis, J. P.; Glaesemann, K. R.; Voth, G. A.; Fritsch, J.; Demkov, A. A.; Ortega, J.; Sankey, O. F. *Phys. Rev. B: Condens. Matter Mater. Phys.* **2001**, *64*, 195103.
(38) Jelnek, J.; Wang, H.; Lewis, J. P.; Sankey, O. F.; Ortega, J. *Phys. Rev. B: Condens. Matter Mater. Phys.* **2005**, *71*, 235101.
(39) Harris, J. *Phys. Rev. B: Condens. Matter Mater. Phys.* **1985**, *31*, 1770.
(40) Foulkes, W.; Haydock, R. *Phys. Rev. B: Condens. Matter Mater. Phys.* **1989**, *39*, 12520.
(41) Sankey, O. F.; Niklewski, D. J. *Phys. Rev. B: Condens. Matter Mater. Phys.* **1989**, *40*, 3979.
(42) Finnis, M. W. *J. Phys.: Condens. Matter* **1990**, *2*, 331.
(43) Wang, H.; Lewis, J. P.; Sankey, O. F. *Phys. Rev. Lett*. **2004**, *93*, 016401.
(44) Wang, H.; Lewis, J. P. *J. Phys. Condens. Matter*. **2005**, *17*, L209.
(45) Becke, A. D. *Phys. Rev. A: At., Mol., Opt. Phys.* **1988**, *38*, 3098.
(46) Yang, C. L. W.; Parr, R. G. *Phys. Rev. B: Condens. Matter Mater. Phys.* **1988**, *37*, 785.
(47) Junquera, J.; Paz, O.; Sánchez-Portal, D.; Artacho, E. *Phys. Rev. B: Condens. Matter Mater. Phys.* **2001**, *64*, 235111.
(48) Kenny, S. D.; Horsfield, A. P.; Fujitani, H. *Phys. Rev. B: Condens. Matter Mater. Phys.* **2000**, *62*, 4899.
(49) Anglada, E.; Soler, J. M.; Junquera, J.; Artacho, E. *Phys. Rev. B: Condens. Matter Mater. Phys.* **2002**, *66*, 205101.
(50) Ozaki, T.; Kino, H. *Phys. Rev. B: Condens. Matter Mater. Phys.* **2004**, *69*, 195113.
(51) Datta, S. *Electronic Transport in Mesoscopic Systems*; Cambridge University Press: Cambridge, 1995.